HHS Public Access

Author manuscript

Exp Eye Res. Author manuscript; available in PMC 2020 March 01.

Published in final edited form as:

Exp Eye Res. 2019 March ; 180: 23–28. doi:10.1016/j.exer.2018.11.027.

INITIATION OF FIBROSIS IN THE INTEGRIN αVβ6 KNOCKOUT MICE

Wenjing Wu[a], **Audrey E.K. Hutcheon**[a], **Sriniwas Sriram**[a], **Jennifer A. Tran**[a], and **James D. Zieske**[a]

[a]Schepens Eye Research Institute/Massachusetts Eye and Ear, Department of Ophthalmology, Harvard Medical School, 20 Staniford Street, Boston, MA 02114. USA. wwj0120@163.com (WW); Audrey_Hutcheon@meei.harvard.edu (AEKH); Sriniwas.sriram@gmail.com (SS); jenntran@bu.edu (JAT); James_Zieske@meei.harvard.edu (JDZ)

Abstract

We previously demonstrated that β6 knockout mice showed impaired wound repair in corneal debridement and keratectomy wounds. In the current investigation, we continued our examination of integrin αvβ6 in order to determine if it was required for the initiation of wound healing in a corneal wound model that normally heals in a fibrotic manner. A full-thickness corneal incision was made in C57BL/6J wild type (WT) and C57BL/6-Itgb6 KO ($\beta6^{-/-}$) mice. The mice were observed at 3, 7, 14, and 28 days post-incision. The morphology of corneal restoration was observed in tissue sections stained with hemotoxilin and eosin (H&E). In addition, indirect-immunofluorescence (IF) was performed on sections and/or whole mounts to evaluate the immunolocalization of α-smooth muscle actin (SMA) and thrombospondin-1 (TSP-1). H&E staining revealed that the corneas in $\beta6^{-/-}$ mice healed slower than those in WT mice, with an obvious delay in the restoration of the stromal matrix and epithelium. In sections at 3 and 7 days, SMA and TSP-1 were greatly reduced in the $\beta6^{-/-}$ mice as compared to WT, but peaked at 28 days after incision. Whole mount SMA IF results were consistent with those from sections. Therefore, the initiation of fibrosis was inhibited by the lack of αvβ6; however, there appeared to be an alternate mechanism that initiated fibrosis 7-14 days later. Localization of TSP-1 correlated with expression of SMA whether wound healing was delayed or initiated immediately after wounding.

Keywords

Fibrosis; wound healing; α-smooth muscle actin; thrombospondin-1; Integrin αVβ6

1. INTRODUCTION

Corneal fibrosis, as well as cell migration, cell proliferation, and matrix remodeling, is an important part of the corneal wound-healing response; however, one of the outcomes of

CORRESPONDING AUTHOR: James D. Zieske, 20 Staniford Street, Boston, MA 02114, USA, James_Zieske@meei.harvard.edu.

fibrosis is an opaque cornea that may impair vision. Fibrosis includes the differentiation of the stromal keratocytes into stress fiber containing cells termed myofibroblasts (Weimar, 1957; Wilson et al., 2003). The stress fibers are formed by α-smooth muscle actin (SMA), which is a known marker of myofibroblasts. These cells, along with the abnormal collagens that they deposit (such as Collagen Type III), block the normal transmission of light through the stroma, thus directly affecting the corneal transparency and reducing visual acuity (Meek and Knupp, 2015). Hence, it is necessary to investigate an efficient way to inhibit fibrosis while still allowing corneal wound healing. One potential method to accomplish this would be to alter the expression of certain integrins.

Integrins are a family of cell surface glycoproteins that function as receptors for extracellular matrix (ECM) proteins, and mediate both cell-substratum and cell-cell adhesion. They are noncovalent, heterodimeric complexes consisting of individual α and β chains (Stepp, 2006). To date there are 18α and 8β subunits which can associate to form at least 24 heterodimers. They can be classified into three major groups: β1, β2, and αv All of the αv containing integrin heterodimers recognize the triple amino acid sequence arginine-glycine-aspartic acid (RGD) in their ligands (Stepp, 2006).

One such ligand for integrin αvβ6 is latent TGF-β1, which is believed to be a major player in corneal fibrosis (Amjad et al., 2007; Carrington et al., 2006; Mamuya and Duncan, 2011; Saika, 2006; Santibanez et al., 2011; Shi et al., 2011; Zavadil and Bottinger, 2005). TGF-β1 is normally secreted in a latent form that must be activated extracellularly to efficiently trigger receptor mediated TGF-β1 signaling. The mature TGF-β1 activity is initially masked by its noncovalent association with a dimer of its N-terminal propeptide, latency-activated peptide (LAP) (Crawford et al., 1998). Integrin αvβ6, has been found to interact with the RGD sequence of latent TGF-β1's LAP, which causes the degradation of LAP (Crawford et al., 1998; Puthawala et al., 2008) and the subsequent dissociation of LAP and TGF-β1, thus activating TGF-β1 and fibrosis (Stepp, 2006), as well as vasculogenesis, immune tolerance, and formation of Langerhans cells (Latella et al., 2013; Puthawala et al., 2008).

Integrin αvβ6 is not expressed in normal conditions; however, upon injury, it is upregulated (Puthawala et al., 2008). Therefore, regulation of integrin αvβ6 could be an attractive therapeutic strategy for fibrosis, as it may be possible to regulate TGF-β at the αvβ6 integrin sites without affecting other vital homeostatic roles of TGF-β. In our previous work, lack of αvβ6 prevents reassembly of the corneal basement membrane (BMZ) and mature hemidesmosomes after keratectomy in β6 knockout ($\beta6^{-/-}$) mice (Morris et al., 2003). Although αvβ6 has been confirmed to mediate TGF-β activation in vivo, determination of integrin αvβ6's precise role in the initiation of corneal fibrosis is still unknown and remains to be clarified.

Latent TGF-β is also activated by thrombospondin 1 (TSP-1), and a recent study of TGF-β1 and TSP-1 knockout mice showed similar patterns of inflammation, suggesting that TSP-1 is a major activator of TGF-β1 in vivo (Munger et al., 1999). TSP-1 is a 450kDa homotrimeric multifunctional ECM glycoprotein (Masli et al., 2014; Uno et al., 2004), which activates TGF-β1 by binding to a defined site on LAP and inducing a conformational change in the latent complex (Mimura et al., 2005; Ribeiro et al., 1999). Previously, we showed that the

localization of SMA-positive cells was in the same area as TSP-1. Interestingly, TSP-1 showed a strikingly selective localization in the wound area and never spread into the stroma outside the original wound area (Matsuba et al., 2011). These results all suggest that TSP-1 may play an important role in TGF-β1 activation and corneal fibrosis; however, the inflammatory changes in the TSP-1 knockout mice are not nearly as severe as those in TGF-β1-knockout mice, suggesting overlapping mechanisms of TGF-β1 activation may be present (Munger et al., 1999). Additionally, the expression of TSP-1 in our previous study was slightly delayed after keratectomy surgery, suggesting that TSP-1 may be downstream of αvβ6 activation of TGF-β1 (Matsuba et al., 2011).

The goal of this study was to determine if αvβ6 is required to initiate fibrosis. To examine this, we compared the expression of SMA after an incisional wound in adult $\beta6^{-/-}$ and wild type (WT) mice. Since β6 only pairs with αv, the $\beta6^{-/-}$ mice result in a functional αvβ6 knockout. Finally, the expression of TSP-1 was also examined during mouse corneal wound healing.

2. MATERIALS AND METHODS

All studies were conducted in accordance with the ARVO Statement for Use of Animals in Ophthalmic and Vision Research and were approved by the IACUC at Schepens Eye Research Institute/Massachusetts Eye and Ear. The 12- to 18-week-old male and/or female C57BL/6J mice (WT: The Jackson Laboratory; Bar Harbor, ME) and C57BL/6-Itgb6 knockout mice ($\beta6^{-/-}$: a kind gift from Dr. Dean Sheppard, University of California; San Francisco, CA) were used in this study. At least three mice were observed per time point per strain.

2.1. Full-Thickness Penetrating Incision

Full-thickness penetrating incision wound was performed as previously described (Blanco-Mezquita et al., 2013). In brief, the WT and $\beta6^{-/-}$ mice were anesthetized, and 1% atropine sulfate ophthalmic solution (Bausch and Lomb, Inc.; Rochester, NY) was instilled in both eyes. Atropine was used to avoid the chronic iris incarceration into the corneal incision. In the right eye, a superior and inferior orientated 1.5mm long full-thickness penetrating incision, which cut all the way through the epithelium, stroma, and endothelium, was created in the center of the cornea with a surgical blade (Fine Science Tools; Foster City, CA). Mice were euthanized 3, 7, 14, and 28 days post-incision, and the whole globe was enucleated and processed for either frozen sectioning or whole mount, with 3-4 eyes/time point/strain. Contralateral eyes were used as unwounded control.

2.2. Frozen Sections

The enucleated whole globes were embedded in liquid OCT compound (Sakura FineTek; Torrance, CA) (Blanco-Mezquita et al., 2013), 10-micron sections were cut with a cryostat (HM 505M, Micron GmbH; Walldorf, Germany) so that a cross-section of the wound area was obtained, and sections were maintained at −20°C until ready to process for either hematoxilin and eosin staining (H&E) (Blanco-Mezquita et al., 2011) or indirect-immunofluorescence (IF) (Blanco-Mezquita et al., 2013).

IF was performed as previously described (Blanco-Mezquita et al., 2013). In brief, tissue sections were washed 3 times in PBS, blocked in 1% BSA (Sigma-Aldrich; St. Louis, MO), and incubated overnight at 4°C with primary antibody—TSP-1 (Abcam; Cambridge, MA) or SMA (Abcam; Cambridge, MA), a marker for myofibroblasts—in 1% BSA + 0.1% Triton-X 100 (Sigma-Aldrich). The next day, sections were washed with PBS and incubated for 1 hour at room temperature with secondary antibody—TRITC-conjugated donkey anti-rabbit IgG (TSP-1) and FITC-conjugated donkey anti-rabbit IgG (SMA: Jackson Immunoresearch; West Grove, PA). Finally, sections were mounted and coverslipped with mounting media (Vectashield: Vector Laboratories; Burlingame, CA) containing DAPI, a marker of all cell nuclei. At least 3 corneas per condition were observed and photographed with a fluorescent microscope (Nikon Eclipse E800; Nikon, Melville, NY). Negative controls, where the primary antibody was omitted, were run with all experiments.

2.3. Whole Mount

Whole globes for whole mount IF were prepared as previously described (Blanco-Mezquita et al., 2011). In brief, whole globes were enucleated, fixed for 2 hours in methanol:dimethyl sulfoxide (4:1), transferred to 100% methanol, and stored at −20°C overnight or until ready for use (Blanco-Mezquita et al., 2011). The corneas were prepared for IF by first isolating the cornea from the globe and then permeabilizing the cornea with methanol:Triton X-100 in the following concentrations and time: 7:3 for 30 minutes, 1:1 for 30 minutes, and 3:7 for 20 minutes (Pal-Ghosh et al., 2004).

Corneas were blocked for 2 hours at room temperature in 3% BSA + 1.5% Triton-X, and then incubated with SMA (1:100) for two days at 4°C. After 2 days, corneas were rinsed 5 × 1 hour (for a total of 5 hours) in PBS at room temperature and incubated overnight with Topro3 (Thermo Fisher scientific; Waltham, MA, USA) and FITC-conjugated donkey anti-rabbit IgG (1:100). Finally, the cornea was flattened on a slide by applying 4 cuts in the peripheral cornea and mounting with mounting media (Vectashield: Vector Labs; Burlingame, CA). Negative controls, where the primary antibody was omitted, were run with all experiments. At least 3 corneas per condition were observed. Images were captured on a confocal microscope (TCS-SP5: Leica Microsystems; Bannockburn, IL).

3. RESULTS

3.1 Tissue morphology

As shown in Figure 1, the unwounded control corneas (Cont) in both WT and $\beta6^{-/-}$ mice looked similar (Fig. 1A and B, respectively). By 3 days post-incision, the epithelium had migrated to cover the wound area in the WT mice (Fig. 1C), and there was a minimal amount of newly synthesized matrix in the stroma. In the $\beta6^{-/-}$ mice (Fig. 1D), the wound gaped open. By 7 days post-incision, the epithelium covering the wound area in the WT mice appeared to be more differentiated as compared to 3 days WT, and new matrix was observed in the stroma (Fig. 1E); however, in the $\beta6^{-/-}$ mice (Fig. 1F), although the epithelium hyperplasia seemed to cover the wound area, there was still a large gap in the stromal wound area, indicating a lack of matrix deposition. By 14 days post-incision, the wound in the WT mice (Fig. 1G) had completely sealed and the epithelium had returned

almost to that seen in control (Fig. 1A). In the stroma, however, a higher number of cells than normal appeared to have accumulated at the wound sight (Fig. 1G). In the $\beta6^{-/-}$ group at 14 days post-incision (Fig. 1H), the epithelium covered the wound area and matrix deposition was apparent. Interestingly, the epithelium and matrix appeared similar to that seen in WT at 7 days post-incision (Fig. 1E). By 28 days, the wound area in both the WT (Fig. 1I) and $\beta6^{-/-}$ (Fig. 1J) mice appeared to be sealed; however, the matrix in the wound area of the WT mice appeared to be disorganized (Fig. 1I). The appearance of the $\beta6^{-/-}$ (Fig. 1J) mice was similar to that seen in WT at 14 days post-incision. Of note, upon wounding, the stroma on either side of the wound site swells because the barrier that normally maintains homeostasis is no longer present. Therefore, over the course of wound healing, the stroma will be of variable thicknesses as observed in Figure 1A compared with Figure 1E.

3.2. TSP-1 expression in the WT and $\beta6^{-/-}$ mice

In order to examine whether knocking out integrin $\alpha v\beta6$ would influence the initiation of wound healing, we examined the localization of TSP-1, an important activator of TGF in wound healing, in WT (Fig. 2A-E) and $\beta6^{-/-}$ (Fig. 2F-J) mice. As shown in Figure 2 in WT mice, no TSP-1 was present in unwounded control corneas (Cont: Fig. 2A); however, at 3 days post-incision (Fig. 2B), TSP-1 appeared in the stromal wound area and extended towards the peripheral cornea, but did not reach the limbus. TSP-1 remained present in the stromal wound area (Fig. 2C, 7 days), but was mostly localized in the wound area and the surrounding tissue. The TSP-1 localization appeared to peak by 14 days post-wounding (Fig. 2D), with the expression of TSP-1 localizing mainly in the stroma subjacent to the wound-healing epithelium. By 28 days post-surgery (Fig. 2E), there was little, if any, TSP-1 present in the wound area.

As with unwounded control corneas of WT mice, no TSP-1 localization appeared to be present in the unwounded control corneas of $\beta6^{-/-}$ mice (Fig. 2F). Upon wounding, low levels of TSP-1 localization appeared near the wound edge at days 3 and 7, with a slight increase at 14 days (Fig. 2G, H, and I, respectively). The TSP-1 localization at these time points, unlike the WT mice, appeared to be distributed in the posterior stroma rather than in the anterior stroma. At 28 days (Fig. 2J), TSP-1 expression seemed to peak in the wound area and its surrounding tissue in a similar manner as in WT mice at 14 days (Fig. 2D). These results suggest that TSP-1 expression was delayed in the $\beta6^{-/-}$ mice compared to the WT mice.

3.3. SMA expression in the WT and $\beta6^{-/-}$ mice

Myofibroblasts, which are characterized by SMA expression, are involved in wound contraction and are a critical component. To see if there was a difference in myofibroblast formation between WT mice and $\beta6^{-/-}$ mice after an incision wound, we observed the localization of SMA by IF in both sections and whole mounts.

3.3.1. Sections—As with TSP-1, SMA showed a similar delay in expression in the $\beta6^{-/-}$ mice (Fig. 3 F-J) as compared with the WT mice (Fig. A-E), reaching maximum expression at 28 days post-incision in the stroma within and immediately adjacent to the wound site. As shown in Figure 3, in the unwound corneas, no SMA staining was detected in either the WT

(Fig. 3A) or $\beta6^{-/-}$ (Fig. 3F) mice. By 3 days after injury, still no SMA was present in either the WT (Fig. 3B) or $\beta6^{-/-}$ (Fig. 3G) mice. At 7 days after surgery, SMA markedly increased in the WT mice (Fig. 3C) and accumulated in the stromal wound site and in the tissue immediately adjacent to the wound site, whereas in the $\beta6^{-/-}$ mice (Fig. 3H), only a small amount of SMA was observed in the wound edge. At day 14, SMA staining reached its peak in WT mice (Fig. 3D), and was present only in the wounded stroma subjacent to the regenerated epithelium. In the $\beta6^{-/-}$ mice (Fig. 3I), more SMA was expressed in the wound area than on day 7 (Fig. 3H), but it was still less than the WT group (Fig. 3D). At day 28 in the WT corneas (Fig. 3E), the SMA expression decreased to almost that seen in unwounded (Fig. 3A); however, in the $\beta6^{-/-}$ mice (Fig. 3J), the SMA staining appeared to reach its highest value, with the staining localizing within the wound area. The intense staining observed in Figure 3E is SMA localization in the iris.

3.3.2. Whole mount—As with the sections, a delay in SMA expression was observed in $\beta6^{-/-}$ mice in the whole mounts. No SMA localization was observed in either unwounded WT (Fig. 4A) or $\beta6^{-/-}$ (Fig. 4F) mice. SMA was expressed at the wound edge in the WT mice at 3 days (Fig. 4B), whereas little, if any, SMA staining was observed in the $\beta6^{-/-}$ mice at this time point (Fig. 4G). On day 7, the SMA expression increased within the stromal wound site and its surrounding tissue in both groups, more SMA staining was found in the WT mice (Fig. 4C) than the $\beta6^{-/-}$ mice (Fig. 4H). On day 14, the SMA expression peaked in the WT mice (Fig. 4D) extending to a larger area within the original wound corresponding to where myofibroblasts would be expected. In the $\beta6^{-/-}$ mice (Fig. 4I), the SMA staining increased, but expression was still lower than the WT mice. By 28 days, the SMA in the WT mice (Fig. 4E) decreased to almost unwounded levels (Fig. 4A); however, the SMA appeared to peak at this time point in the $\beta6^{-/-}$ mice (Fig. 4J).

4. DISCUSSION

This study examined if $\alpha v\beta6$ was required for the initiation of fibrosis in the cornea after a wound. Previously, we demonstrated that laminin production during wound repair was reduced and healing rate after a keratectomy wound was slowed in $\beta6^{-/-}$ mice (Desgrosellier and Cheresh, 2010). In addition, we demonstrated that TSP-$1^{-/-}$ mice showed greatly impaired healing (Blanco-Mezquita et al., 2013), and in the current study, we found that penetrating wounds in $\beta6^{-/-}$ mice exhibit prolonged gaping, similar to that seen in the TSP-$1^{-/-}$ mice (Blanco-Mezquita et al., 2013). Since both knockout mice show a similar phenotype after wounding and both $\alpha v\beta6$ and TSP-1 are known to activate TGF-β1, we postulated that there is a link between $\alpha v\beta6$ and TSP-1.

In a corneal wound, active TGF-β is upregulated, and in corneal fibrosis, TGF-β acts as a master profibrogenic cytokine by promoting mesenchymal cells to synthesize ECM (Crawford et al., 1998). Continuous TGF-β signaling stimulates quiescent keratocytes adjacent to the injury to transition into activated fibroblasts and myofibroblasts. In order for this to occur, TGF-β must be activated, and it has been shown that both $\alpha v\beta6$ and TSP-1 activate TGF-β1 by binding the LAP of the latent TGF-β1 complex (Crawford et al., 1998; Puthawala et al., 2008; Ribeiro et al., 1999; Stepp, 2006). Upon wounding, both TGF-β1 (Carrington et al., 2006) and $\alpha v\beta6$ (Blanco-Mezquita et al., 2011) are upregulated in the

wound area, which presents the increased amount of αvβ6 with the opportunity to activate the increased levels of TGF-β1 (Blanco-Mezquita et al., 2011; Blanco-Mezquita et al., 2013). This presents the question if αvβ6 is knocked out will the amount of activated TGF-β1 be reduced? If this is the case, then myofibroblast differentiation, especially at the early stages of wound healing will be inhibited. Interestingly, this appears to be the case, for the data from the present study shows that early in the wound healing processes (3 and 7 days), $\beta6^{-/-}$ mouse corneas were slow to heal, had gaping wounds (Fig. 1D,F), and little, if any, SMA (Fig. 3G,H and 4G,H); however, WT mouse corneas healed by day 3, with newly repaired or synthesized matrix (Fig. 1C) and by day 7 had large amounts of SMA localizing in the wound area (Fig. 3C, 4C). This lack of SMA localization observed in the $\beta6^{-/-}$ mice may be responsible for the gaping wound since myofibroblasts are involved in contracting tissue to close the wound and depositing ECM in the wound area. However, corneal wound healing in $\beta6^{-/-}$ mice was not completely inhibited, only delayed; therefore, there must be other factors that play a role in this process.

One such factor may be TSP-1, since in addition to activating TGF-β1 after wounding, the upregulated αvβ6 also stimulated an increase in TSP-1 (Fig. 2A-E), suggesting that TSP-1 is downstream of αvβ6 and presumably mediated by TGF-β1 In addition to being activated by αvβ6, TSP-1 has been found to co-localize with SMA in the stroma after wounding and be involved in the transformation of keratocytes into myofibroblasts (Matsuba et al., 2011). Initially, the wound-healing process in the $\beta6^{-/-}$ mice was slow and little TSP-1 was localized in the wound area (Fig. 2G,H); however, at later time points, deposition of TSP-1 became increasingly apparent (Fig. 2I,J). In order for this to happen, it must have occurred by a non-αvβ6 mechanism, which allowed for TGF-β1 expression and fibrosis. This agrees with the increased amount of myofibroblasts that appeared in the $\beta6^{-/-}$ mice, particularly at 28 days (Fig. 3I,J and 4I,J). These data suggest that TSP-1 may serve to amplify the activation of TGF-β by αvβ6, and TSP-1 appears to be at least partially dependent on the presence of αvβ6 since it was significantly reduced in the $\beta6^{-/-}$ mice at early stages. Therefore, Integrin αvβ6 may activate TGF-β1 in the stromal cells via TSP-1.

The fact that after the penetrating incision the $\beta6^{-/-}$ mice healed slower with reduced SMA and TSP-1 indicates that treatment with anti-αvβ6 monoclonal antibodies may be beneficial clinically to slow the healing process to attenuate the scar formation. However, our findings underscore the difficulty with developing a therapeutic anti-fibrotic treatment, which is currently limited (Henderson and Sheppard, 2013). For even though αvβ6 is involved in rapid activation of wound healing, an alternate, slower pathway(s) is(are) also available. There have been studies that used a blocking antibody to αvβ6 that was able to reduce bleomycin induced increases in collagen expression in a dose-dependent manner (Wilson and Wynn, 2009). Of interest will be the long-term studies, which may demonstrate that this effect is just delayed rather than blocked. Indeed, inhibition of αvβ6 offers the possibility of local inhibition of TGF-β1 without affecting other homeostatic roles of TGF-β1; however, other pathways to activate TGF-β must also be examined. Therefore, more studies with larger sample size, longer observation time, and quantification data are required to consolidate the results and determine whether these findings can be translated to a useful long-term therapeutic.

5. CONCLUSION

The integrin αvβ6 appears to be necessary to quickly initiate fibrosis, since knocking out αvβ6 reduced the expression of SMA and TSP-1 at the early stage of the wound-healing process. Our data suggests that αvβ6 may initiate the process, while TSP-1 provides a method of amplification. Therefore, blocking the action of the integrin αvβ6 or TSP-1 through the use of antibodies or small molecule inhibitors may be considered as a specific treatment of scarring corneal diseases.

ACKNOWLEDGMENTS

This study was funded by grants from National Institute of Health (EY03790 and EY005665). Authors have no commercial interests to disclose.

REFERENCES

Amjad SB, Carachi R, Edward M, 2007 Keratinocyte regulation of TGF-beta and connective tissue growth factor expression: a role in suppression of scar tissue formation. Wound Repair Regen 15, 748–755. [PubMed: 17971021]

Blanco-Mezquita JT, Hutcheon AE, Stepp MA, Zieske JD, 2011 alphaVbeta6 integrin promotes corneal wound healing. Investigative ophthalmology & visual science 52, 8505–8513. [PubMed: 21960555]

Blanco-Mezquita JT, Hutcheon AE, Zieske JD, 2013 Role of thrombospondin-1 in repair of penetrating corneal wounds. Investigative ophthalmology & visual science 54, 6262–6268. [PubMed: 23963165]

Carrington LM, Albon J, Anderson I, Kamma C, Boulton M, 2006 Differential regulation of key stages in early corneal wound healing by TGF-beta isoforms and their inhibitors. Investigative ophthalmology & visual science 47, 1886–1894. [PubMed: 16638995]

Crawford SE, Stellmach V, Murphy-Ullrich JE, Ribeiro SM, Lawler J, Hynes RO, Boivin GP, Bouck N, 1998 Thrombospondin-1 is a major activator of TGF-beta1 in vivo. Cell 93, 1159–1170. [PubMed: 9657149]

Desgrosellier JS, Cheresh DA, 2010 Integrins in cancer: biological implications and therapeutic opportunities. Nature reviews. Cancer 10, 9–22.

Henderson NC, Sheppard D, 2013 Integrin-mediated regulation of TGFbeta in fibrosis. Biochimica et biophysica acta 1832, 891–896. [PubMed: 23046811]

Latella G, Vetuschi A, Sferra R, Speca S, Gaudio E, 2013 Localization of alphanubeta6 integrin-TGF-beta1/Smad3, mTOR and PPARgamma in experimental colorectal fibrosis. European journal of histochemistry : EJH 57, e40. [PubMed: 24441193]

Mamuya FA, Duncan MK, 2011 alphaV integrins and TGF-beta induced EMT; a circle of regulation. J Cell Mol Med.

Masli S, Sheibani N, Cursiefen C, Zieske J, 2014 Matricellular protein thrombospondins: influence on ocular angiogenesis, wound healing and immuneregulation. Current eye research 39, 759–774. [PubMed: 24559320]

Matsuba M, Hutcheon AE, Zieske JD, 2011 Localization of thrombospondin-1 and myofibroblasts during corneal wound repair. Experimental eye research 93, 534–540. [PubMed: 21749870]

Meek KM, Knupp C, 2015 Corneal structure and transparency. Progress in retinal and eye research 49, 1–16. [PubMed: 26145225]

Mimura Y, Ihn H, Jinnin M, Asano Y, Yamane K, Tamaki K, 2005 Constitutive thrombospondin-1 overexpression contributes to autocrine transforming growth factor-beta signaling in cultured scleroderma fibroblasts. The American journal of pathology 166, 1451–1463. [PubMed: 15855645]

Morris DG, Huang X, Kaminski N, Wang Y, Shapiro SD, Dolganov G, Glick A, Sheppard D, 2003 Loss of integrin alpha(v)beta6-mediated TGF-beta activation causes Mmp12-dependent emphysema. Nature 422, 169–173. [PubMed: 12634787]

Munger JS, Huang X, Kawakatsu H, Griffiths MJ, Dalton SL, Wu J, Pittet JF, Kaminski N, Garat C, Matthay MA, Rifkin DB, Sheppard D, 1999 The integrin alpha v beta 6 binds and activates latent TGF beta 1: a mechanism for regulating pulmonary inflammation and fibrosis. Cell 96, 319–328. [PubMed: 10025398]

Pal-Ghosh S, Pajoohesh-Ganji A, Brown M, Stepp MA, 2004 A mouse model for the study of recurrent corneal epithelial erosions: alpha9beta1 integrin implicated in progression of the disease. Investigative ophthalmology & visual science 45, 1775–1788. [PubMed: 15161840]

Puthawala K, Hadjiangelis N, Jacoby SC, Bayongan E, Zhao Z, Yang Z, Devitt ML, Horan GS, Weinreb PH, Lukashev ME, Violette SM, Grant KS, Colarossi C, Formenti SC, Munger JS, 2008 Inhibition of integrin alpha(v)beta6, an activator of latent transforming growth factor-beta, prevents radiation-induced lung fibrosis. American journal of respiratory and critical care medicine 177, 82–90. [PubMed: 17916808]

Ribeiro SM, Poczatek M, Schultz-Cherry S, Villain M, Murphy-Ullrich JE, 1999 The activation sequence of thrombospondin-1 interacts with the latency-associated peptide to regulate activation of latent transforming growth factor-beta. The Journal of biological chemistry 274, 13586–13593. [PubMed: 10224129]

Saika S, 2006 TGFbeta pathobiology in the eye. Lab Invest 86, 106–115. [PubMed: 16341020]

Santibanez JF, Quintanilla M, Bernabeu C, 2011 TGF-beta/TGF-beta receptor system and its role in physiological and pathological conditions. Clin Sci (Lond) 121,233–251. [PubMed: 21615335]

Shi M, Zhu J, Wang R, Chen X, Mi L, Walz T, Springer TA, 2011 Latent TGF-beta structure and activation. Nature 474, 343–349. [PubMed: 21677751]

Stepp MA, 2006 Corneal integrins and their functions. Experimental eye research 83, 3–15. [PubMed: 16580666]

Uno K, Hayashi H, Kuroki M, Uchida H, Yamauchi Y, Kuroki M, Oshima K, 2004 Thrombospondin-1 accelerates wound healing of corneal epithelia. Biochemical and biophysical research communications 315, 928–934. [PubMed: 14985101]

Weimar V, 1957 The transformation of corneal stromal cells to fibroblasts in corneal wound healing. American journal of ophthalmology 44, 173–180; discussion 180-172. [PubMed: 13469964]

Wilson MS, Wynn TA, 2009 Pulmonary fibrosis: pathogenesis, etiology and regulation. Mucosal immunology 2, 103–121. [PubMed: 19129758]

Wilson SE, Mohan RR, Hutcheon AE, Mohan RR, Ambrosio R, Zieske JD, Hong J, Lee J, 2003 Effect of ectopic epithelial tissue within the stroma on keratocyte apoptosis, mitosis, and myofibroblast transformation. Experimental eye research 76, 193–201. [PubMed: 12565807]

Zavadil J, Bottinger EP, 2005 TGF-beta and epithelial-to-mesenchymal transitions. Oncogene 24, 5764–5774. [PubMed: 16123809]

HIGHLIGHTS

- $\beta6^{-/-}$ mouse corneas healed slower than WT mice.
- SMA and TSP-1 was greatly reduced in $\beta6^{-/-}$ mouse corneas at early time points.
- At later time points SMA and TSP-1 increased and peaked 28 days post-incision.
- The initiation of fibrosis was inhibited by the lack of $\alpha v\beta6$.
- An alternate mechanism in $\beta6^{-/-}$ mice initiated fibrosis 7-14 days later than in WT.

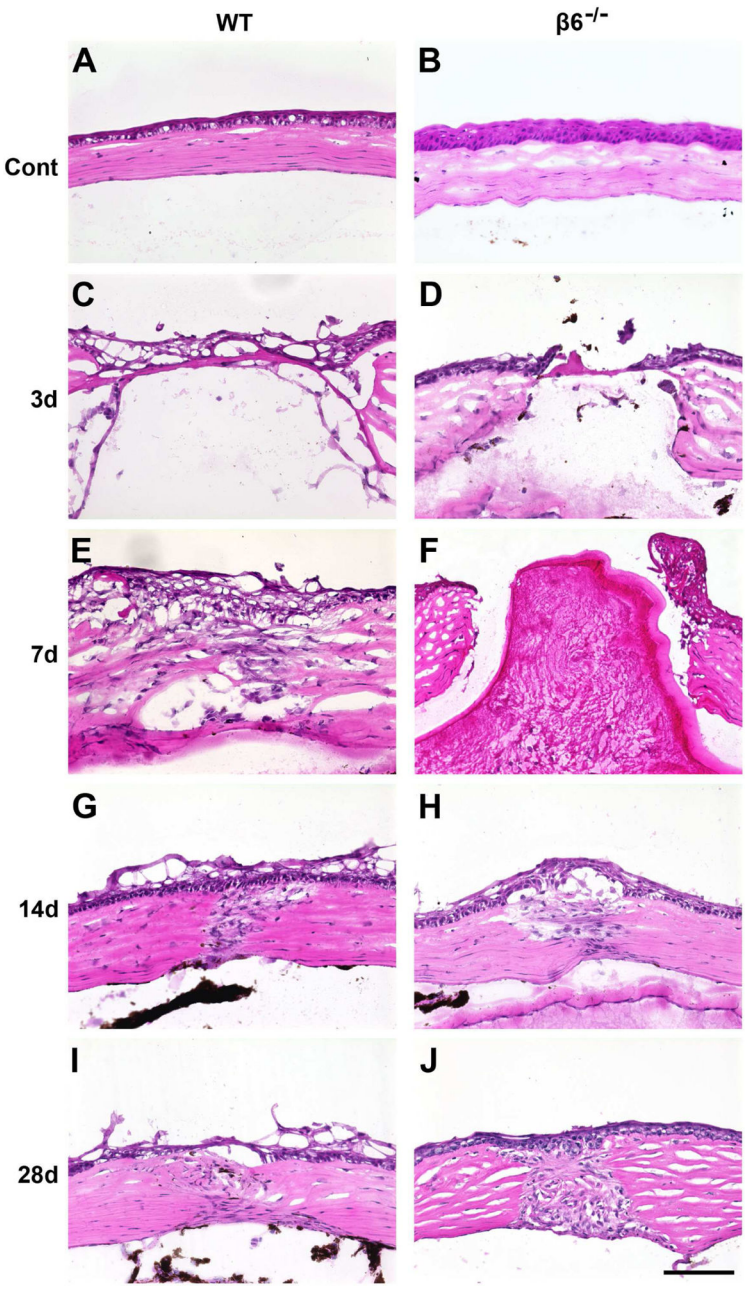

Figure 1:

Representative H&E images of the WT (A, C, E, G, and I) and β6$^{-/-}$ (B, D, F, H, and J) mice before (Cont: A, B) and 3 (C, D), 7 (E, F), 14 (G, H), and 28 (I, J) days (d) after incision wound. Bar = 100μm.

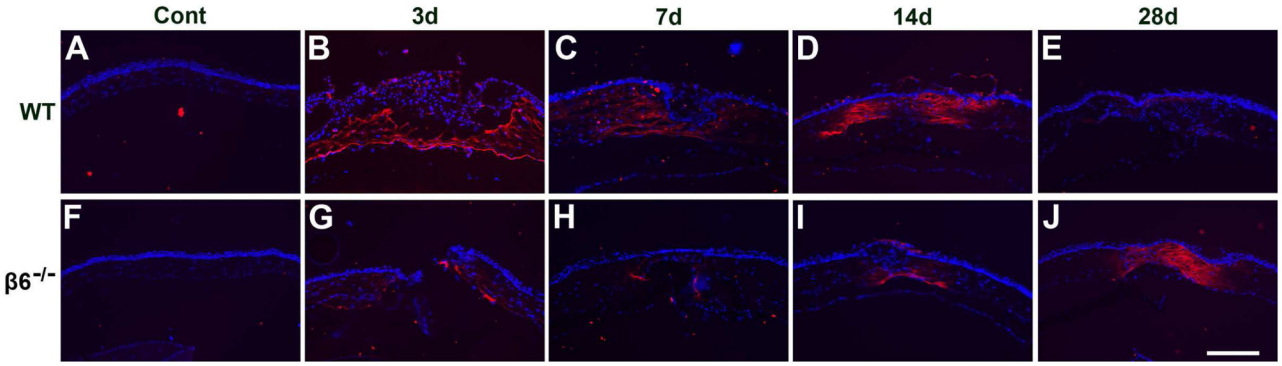

Figure 2:

Representative IF images of TSP-1 (red) localization in the WT (A-E) and $\beta 6^{-/-}$ (F-J) mice before (Cont: A, F) and 3 (B, G), 7 (C, H), 14 (D, I), and 28 (E, J) days (d) after incision wound. Blue = DAPI, a nuclear counterstain. Bar = 200μm.

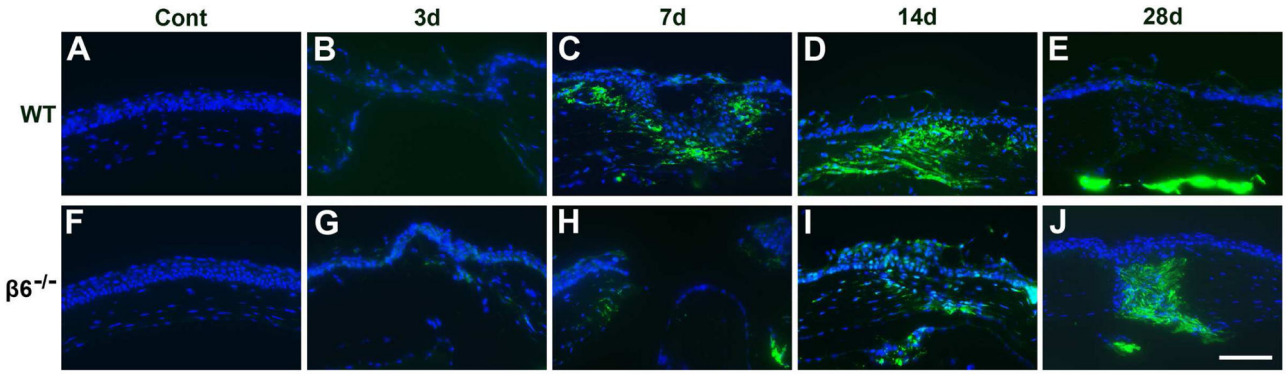

Figure 3:

Representative IF images of SMA (green) localization in the WT (A-E) and $\beta 6^{-/-}$ (F-J) mice before (Cont: A, F) and 3 (B, G), 7 (C, H), 14 (D, I), and 28 (E, J) days (d) after incision wound. Blue = DAPI, a nuclear counterstain. Bar = 100μm.

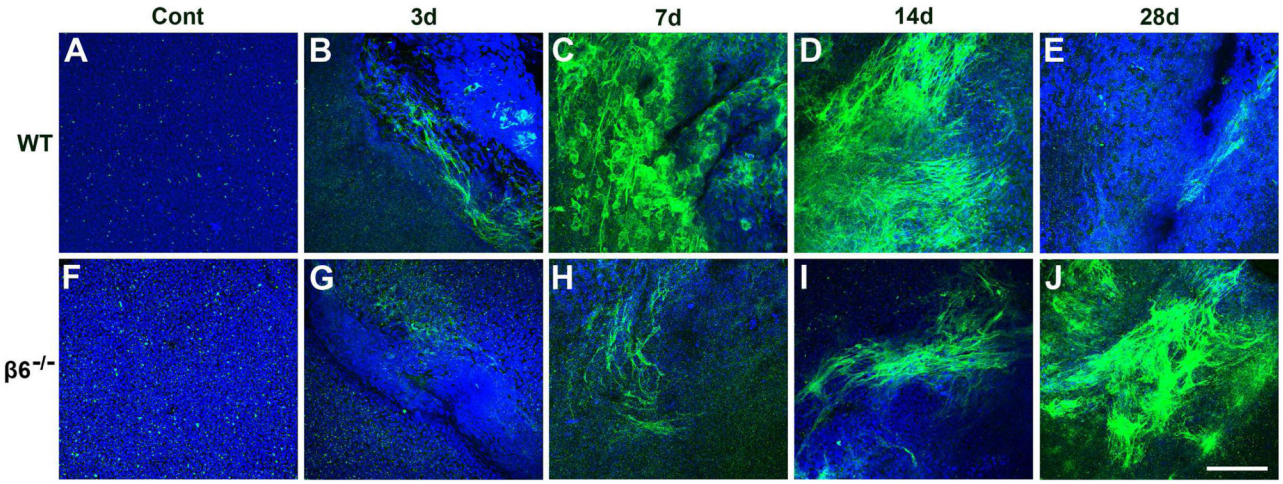

Figure 4:

Representative whole mount maximum projection confocal IF images of SMA (green) localization in the WT (A-E) and $\beta6^{-/-}$ (F-J) mice before (Cont: A, F) and 3 (B, G), 7 (C, H), 14 (D, I), and 28 (E, J) days (d) after incision wound. Blue = DAPI, a nuclear counterstain. Bar = 100μm.